Nano Research
2021, 14(2): 417–422
ISSN 1998-0124 CN 11-5974/O4
https://doi.org/10.1007/s12274-020-3123-z

Research Article

Applying reticular synthesis to the design of Cu-based MOFs with mechanically interlocked linkers

Alexander J. Stirk[1], Benjamin H. Wilson[1], Christopher A. O'Keefe[1], Hazem Amarne[2], Kelong Zhu[3], Robert W. Schurko[4], and Stephen J. Loeb[1] (✉)

[1] *Department of Chemistry and Biochemistry, University of Windsor, Windsor, Ontario, N9B 3B4, Canada*
[2] *Department of Chemistry, The University of Jordan, Amman, 11942, Jordan*
[3] *School of Chemistry, Sun Yat-Sen University, Guangzhou 510275, China*
[4] *Department of Chemistry and Biochemistry, Florida State University, Tallahassee, Florida 32306-4390, USA*

Received: 19 August 2020 / **Revised:** 12 September 2020 / **Accepted:** 14 September 2020

ABSTRACT

The concept of "robust dynamics" describes the incorporation of mechanically interlocked molecules (MIMs) into metal-organic framework (MOF) materials such that large amplitude motions (e.g., rotation or translation of a macrocycle) can occur inside the free volume pore of the MOF. To aid in the preparation of such materials, reticular synthesis was used herein to design rigid molecular building blocks with predetermined ordered structures starting from the well-known MOF **NOTT-101**. New linkers were synthesized that have a T-shape, based on a triphenylene tetra-carboxylate strut, and their incorporation into Cu(II)-based MOFs was investigated. The single-crystal structures of three new MOFs, **UWCM-12** (fof), β-**UWCM-13** (loz), **UWCM-14** (lil), with naked T-shaped linkers were determined; β-**UWCM-13** is the first reported example of the loz topology. A fourth MOF, **UWDM-14** (lil) is analogous to **UWCM-14** (lil) but contains a [2]rotaxane linker. Variable-temperature, ^{2}H solid-state NMR was used to probe the dynamics of a 24-membered macrocycle threaded onto the MOF skeleton.

KEYWORDS

reticular chemistry, metal-organic frameworks, mechanically interlocked molecules, rotaxane

1 Introduction

While there are a wealth of innovative molecular switches and machines based on mechanically interlocked molecules (e.g., rotaxanes, catenanes) that operate in solution [1–6], transferring their motion to the solid-state requires additional design features [7, 8]. Components with both rigid and flexible structures are needed such that the mobile (flexible) units can be placed within or tethered to an ordered (rigid) skeletal structure. The term "robust dynamics" was coined by Stoddart and Yaghi to describe incorporating mechanically interlocked molecules (MIMs) into metal-organic frameworks (MOFs) [9]. Although a few examples of MIMs in MOFs [10–18] have been reported, to reliably create a material exhibiting robust dynamics, some degree of predictability in design is desirable. Reticular synthesis—the process of assembling judiciously designed rigid molecular building blocks into predetermined ordered structures—seems ideal for this purpose [19]. Herein, we describe this concept using the iconic material **NOTT-100** as a starting point, followed by synthesis of MIM linkers for incorporation into related MOFs (Fig. 1) [20].

MOF materials in the **UWDM** (University of Windsor Dynamic Material) series have provided significant progress towards achieving the goal of robust dynamics but have fallen short of providing rational design parameters [10–12, 14–17]. In the case of **UWDM-1** (Fig. 1(b)), an fof net was formed and rotation of the macrocyclic ring inside the MOF was characterized by variable temperature (VT) ^{2}H solid-state NMR (SSNMR) [16]. However, when the interlocked macrocycle was not present, as in **UWCM-1** (University of Windsor Crystalline Material), the resulting structure has a unique topology containing a complex rhombihexahedron interconnected with large cuboctahedral cages (nanoballs) [14]. The organic backbones of the two linkers are identical but, when the wheel is interlocked around the axle, it adds rigidity. A reticular approach to linker design might avoid these pitfalls while not compromising the ultimate goal of creating robust dynamics.

For **NOTT-101** (Fig. 1(c)), the carboxylates of the linker coordinate to Cu(II) ions creating a 4-connected dicopper paddlewheel secondary building unit (SBU) resulting in an fof net [20]. The fof net is typified by two cages within the MOF structure; a hexagonal cage [$Cu_{12}L_{12}$] and an elongated [$Cu_{24}L_{6}$] cage that provides the **NOTT-100** series with high porosity and affinity for H_2 adsorption [20–22]. The linker is open to synthetic decoration at the central phenyl ring (Fig. 1(d), **ZJU-7**) [23], making it amenable to reticular synthesis and a good target for incorporating T-shaped [2]rotaxane linkers [24] and their "naked axle" (i.e. without the interlocked wheel) analogs.

2 Results and discussion

2.1 T-shaped linkers based on NOTT-100

T-shaped triphenyl diisophthalic linkers were designed and

Address correspondence to loeb@uwindsor.ca

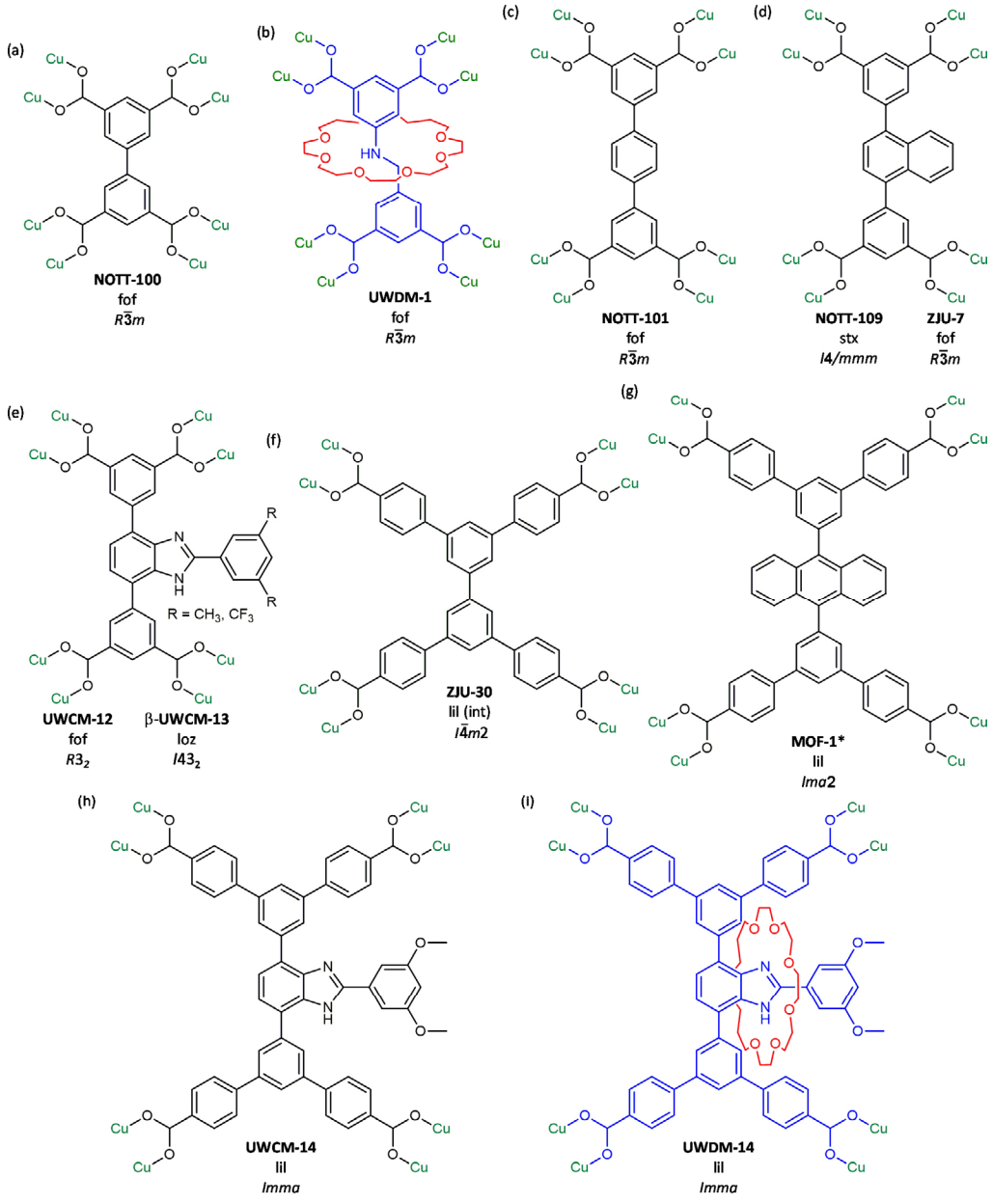

Figure 1 The reticular design of T-shaped linkers and their mechanically interlocked (rotaxane) analogs. (a) A diphenyl strut is used to make **NOTT-100**. (b) A [2]rotaxane linker is used to make **UWDM-1**; denoted **UWCM-1** without the macrocycle. (c) A triphenyl strut is used to make **NOTT-101**. (d) A naphthyl-containing strut is used to make **NOTT-109**. (e) A T-shaped strut is used to make new MOFs **UWCM-12**, α-**UWCM-13** and β-**UWCM-13**. (f) and (g) Extended struts are used to make **ZJU-30** and **MOF-1*** (*Mukherjee). (h) An extended T-shaped strut is used to make new MOF **UWCM-14** and (i) a T-shaped MIM is used to make the MIM in MOF **UWDM-14**.

prepared (Scheme 1); i.e., naked T-shaped linkers **3a** (R = CH_3) and **3b** (R = CF_3) and in one case the analogous [2]rotaxane **3b⊂24C6**. The three linkers were synthesized from the diamine precursor **1** by condensation with the appropriate aldehyde to yield tetraesters **2a** and **2b**. The esters were easily hydrolyzed to the naked axles **3a** and **3b**. To create the [2]rotaxane, **2b** was protonated using HBF_4 and the resulting benzimidazolium cation used as the template in a ring-closing metathesis (RCM) reaction with a crown ether precursor [25], followed by reduction using $^2H_2$(g) to yield the [2]rotaxane **2b⊂24C6**. This could then be hydrolyzed to create [2]rotaxane linker **3b⊂ 24C6**. The incorporation of deuterium labels allows for the potential monitoring of macrocycle dynamics (e.g., rotation) inside a MOF using VT ^{2}H SSNMR. The axle **2a** was not suitable for the synthesis of the analogous rotaxane linker **2a⊂24C6** as the methyl groups were found to provide insufficient bulk to prevent dethreading of the macrocycle.

No dethreading was observed for **3b⊂24C6** during ester hydrolysis so it was concluded that trifluoromethyl groups (R = CF_3) are suitably sized stoppers for this type of T-shaped [2]rotaxane containing a **24C6** ring. All new linkers and their precursors were fully characterized by standard ^{1}H and ^{13}C NMR experiments as well as high-resolution mass spectrometry; **2b** and **2b⊂24C6** were also characterized by single-crystal X-ray diffraction (SCXRD) (see the Electronic Supplementary Material (ESM) for full details of synthesis and characterization).

2.2 MOFs UWCM-12, α- and β-UWCM-13

Three new Cu(II) MOFs were successfully synthesized and characterized using the two naked linkers **3a** and **3b** (Fig. 1(e); see the ESM for details of MOF synthesis). The MOF produced utilizing **3a** was designated **UWCM-12**, while **3b** yielded two separate phases, the major product was designated α-**UWCM-13**

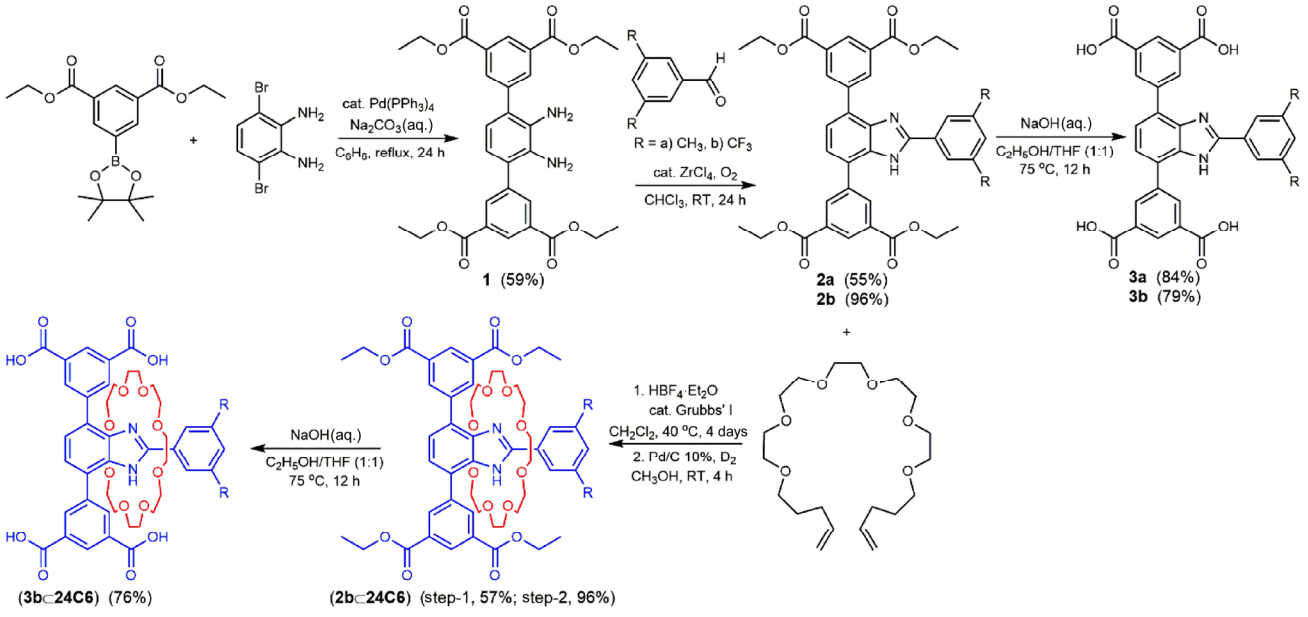

Scheme 1 Synthetic steps used to prepare T-shaped axles and [2]rotaxane linkers with a triphenylene strut and isophthalic groups.

and the minor phase β-**UWCM-13** [26]. Unfortunately, no crystalline material could be isolated when employing [2]rotaxane, **3b⊂24C6** (R = CF_3) as a linker. This could be attributed to the increased steric bulk, imposed by the macrocycle, relatively close to the coordinating isophthalate groups making it an unsuitable ligand for synthesizing MOFs.

UWCM-12 was synthesized under solvothermal conditions producing large green rhomboid crystals (Fig. S1 in the ESM). Analysis by SCXRD revealed a MOF framework with square planar Cu(II) paddlewheel SBUs in the trigonal space group $R3_2$ (Fig. 2). The central benzimidazole moiety is disordered over two positions but the aromatic substituents at the 2-postion are too sterically hindered to point towards one another and therefore must be oriented in an alternating manner. It is also evident that a maximum of three substituents can simultaneously occupy each cavity and that the units cannot point into the $[Cu_{24}L_6]$ cage. Analysis using Olex2 [27] solvent mask (Olex2 implementation of the Platon Squeeze routine [28]) revealed a total solvent accessible void space (1.2 Å probe) of 6,884 $Å^3$ (59%). The resulting fof net is the same as observed for **ZJU-7** [23] which contains a central naphthalene moiety and is in contrast to the ssb net reported for **NOTT-109** (Fig. 1(d)) [20]. Despite rapid mass loss at room temperature of the as-synthesized **UWCM-12** as shown via thermal gravimetric analysis (TGA), the framework integrity was maintained up to 175 °C as shown via powder X-ray diffraction (PXRD) for the activated **UWCM-12**.

Linker **3b** (R = CF_3), when reacting under solvothermal conditions with a Cu(II) source, produced two phases denoted α-**UWCM-13** and β-**UWCM-13**. The bulk of the microcrystalline material (α-**UWCM-13**) was shown by PXRD (Fig. S6 in the ESM) to adopt an fof net analogous to **UWCM-12**. More interestingly, a small amount of large, odd-shaped crystals (Fig. S5 in the ESM) of β-**UWCM-13** suitable for SCXRD analysis could be physically separated from the bulk phase. The structure of β-**UWCM-13** is remarkable in terms of size and aesthetics (Fig. 3(a)). β-**UWCM-13** features a new net denoted loz and is a new entry to the Topos Topological Types Database [29, 30]. The most significant feature of the framework is a large central cavity with a Cu···Cu distance measuring ~ 38 Å; larger than the Zr···Zr distance of ~ 36 Å across the hexagonal pores of **NU-1000** [31]. The CF_3 groups line the walls of this large cavity and the formation of β-**UWCM-13** may be due to some type

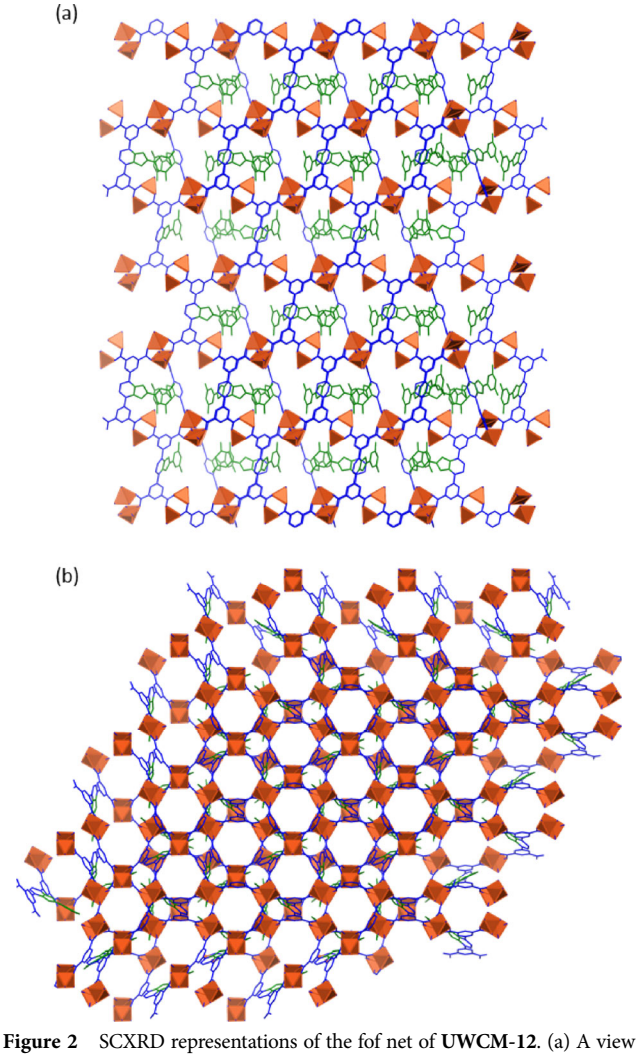

Figure 2 SCXRD representations of the fof net of **UWCM-12**. (a) A view down the a-axis showing the orientation of the benzimidazole fragment (green) into the pores, (b) a view down the c-axis emphasizing the hexagonal channels.

of hydrophobic aggregation. Analysis using the Olex2 solvent mask reveals a solvent accessible void space (1.20 Å probe) of 88,384 $Å^3$ (65%). However, due to the disorder benzimidazole

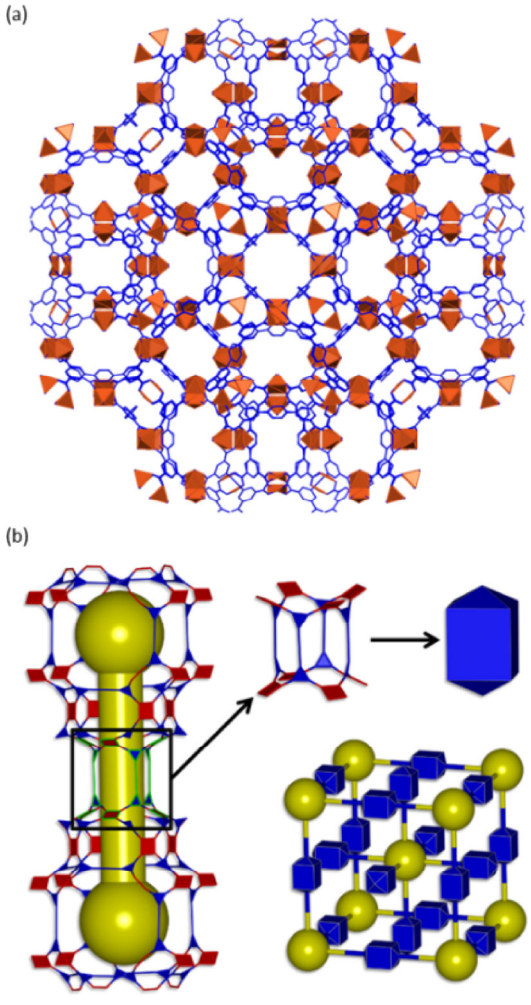

Figure 3 SCXRD representation of the loz net of β-**UWCM-13**. (a) A view down the c-axis, the disordered benzimidazole fragments are omitted for clarity. (b) A visualization of the connectivity of the representative void space in β-**UWCM-13** showing octahedral like pores further linked by nano channels.

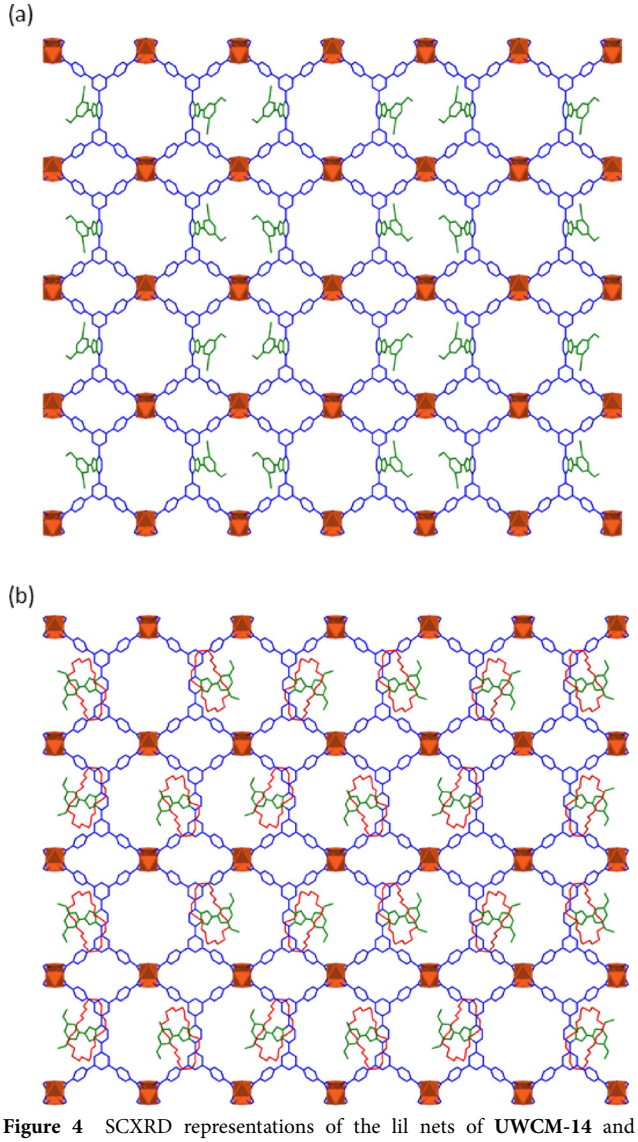

Figure 4 SCXRD representations of the lil nets of **UWCM-14** and **UWDM-14**. (a) A view down the a-axis of **UWCM-14**, (b) a view down the a-axis of **UWDM-14**.

groups, the actual porosity of the framework is quite limited [32]. Small 11.2 Å wide 'nano-channels' made up of $Cu_{16}L_4$ cages link the large individual cavities (Fig. 3(b)). The large individual cavities are arranged in that can be described as a body centered cubic (BCC) fashion with each cavity linked to six others via the aforementioned "nano-channels" (Fig. 4) reminiscent of the rho topological net observed in zeolites [33] and ZIFs [34]. What differentiates the loz net is that it is composed of two independent rho-like pore structures which are interpenetrated. Unfortunately, multiple attempts to create this new loz net with the [2]rotaxane linker, **3b⊂24C6,** did not produce an analogous framework, potentially due to the increased steric bulk imposed by the macrocycle.

2.3 New T-shaped linkers via reticular synthesis

Since the nbo derived nets did not create a cavity sufficiently porous enough to accommodate a large moiety (with or without an interlocked macrocycle) perpendicular to the triphenyl backbone, it was decided to expand, in a reticular fashion, the breadth of the linker by inserting extra phenyl groups between the triphenyl strut and the isophthalic acid group. This basic linker design has been used by Mukerjee [35] to create a Cu(II)-based MOF (**MOF-1**) with a derived lil net, from the parent lvt net, while a similar biphenylene linker produced **ZJU-30** which has an interpenetrated lil net [36, 37]. Additionally, methoxy (OMe) groups were used on the stoppering unit as they are suitably bulky enough to prevent dethreading and eliminate the formation of MOF structures likely driven by hydrophobicity (CF_3) (see Fig. 1 for details of these linkers and MOFs and Scheme 2 for the syntheses of the new linkers **7** and **7⊂24C6)**.

Preparation of the axle was initiated using a $ZrCl_4$ catalyzed condensation reaction between 3,6-dibromobenzene-1,2-diamine and 3,5-dimethoxy-benzaldehyde, resulting in benzimidazole **4**. To obtain naked linker **7**, **4** was enlarged using a Suzuki coupling reaction with diethyl-5'-(4,4,5,5-tetramethyl-1,3,2-dioxaborolan-2-yl)-[1,1':3',1''-terphenyl]-4,4''-dicarboxylate, followed by hydrolysis with NaOH. The [2]rotaxane synthon **4⊂24C6** was prepared by protonating **4** with $HBF_4{\cdot}Et_2O$ to yield a template for pre-crown, pentaethyleneglycol-dipent-4-enyl and the mechanical bond was formed through RCM using Grubbs' 1st generation catalyst [25]. The **24C6** wheel is mechanically locked by two Br substituents on one end of the axle and two methoxy substituents on the other. The RCM reaction produces both *E* and *Z* isomers, which were not separated to maximize percentage recovery. [2]Rotaxane **4⊂24C6** was then extended to yield **6⊂24C6** via another Suzuki coupling which was followed by hydrogenation using Pd/C catalysis with $^2H_2$ (D_2). Finally, hydrolysis using NaOH created the tetra-acid [2]rotaxane linker **7⊂24C6**.

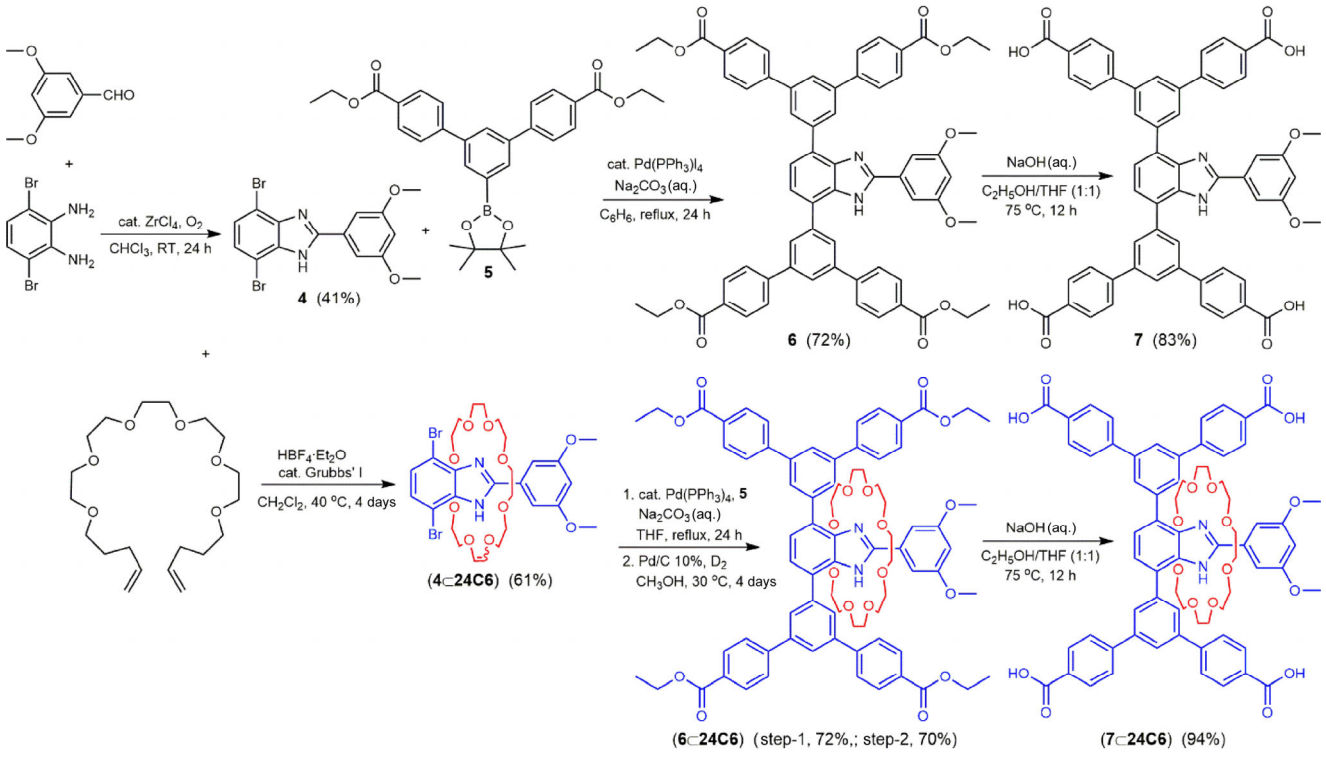

Scheme 2 Synthetic steps used to prepare T-shaped axles and [2]rotaxane linkers with extended struts and isophthalic groups.

2.4 MOFs UWCM-14 and UWDM-14

MOFs **UWCM-14** and **UWDM-14** were produced through solvothermal synthesis with Cu(II) ions employing linkers **7** and **7⊂24C6**, respectively. Both MOFs are isolated as large green single crystals (Fig. S8 in the ESM) and the as-synthesized materials were subjected to X-ray diffraction. Figure 5 shows that both **UWCM-14** and **UWDM-14** adopt the targeted non-interpenetrated lil net found for Mukerjee's MOF-1 [35]. **UWCM-14** shows a 50:50 occupancy, two site positional disorder of the central benzimidazole moiety, with a dihedral angle of 43.0(4)°. **UWDM-14** displays the same 50:50 occupational disorder, but with a 45.7(9)° dihedral angle, showing that the presence of the wheel has a minor effect on the local structure, but not the overall net. VT-PXRD (Figs. S9 and S13 in the ESM) showed that both frameworks are stable when activated up to 175 °C without any noticeable phase changes or loss of crystallinity. Analysis using Olex2 solvent mask (1.2 Å probe) reveals a solvent accessible void of 11,539 Å^3 (73%) for **UWCM-14**. Upon incorporation of the **24C6** macrocyclic wheel in **UWDM-14**, a significant decrease in the solvent accessible volume is observed to 5,873 Å^3 (41%).

The dynamics of the ^{2}H labelled mechanically interlocked macrocycle was probed using ^{2}H VT SSNMR spectroscopy. Although magnetically dilute, the Cu(II) paddlewheel SBUs are paramagnetic and this resulted an efficient T_2 relaxation of the ^{2}H nuclei, which led to patterns with low signal-to-noise ratios and asymmetric shapes resulting from dipolar shift anisotropy (Fig. S19(a) and discussion in the ESM). Although this prevented accurate molecular modelling of the motion in **UWDM-14**, the experimental spectra infer that the same types of rocking, partial rotation, and perhaps full rotational motion (Figs. S19(b) and S19(c) in the ESM) identified for related MOFs **UWDM-1** [16], **UWDM-2** [15], **UWDM-3** [15], **UWDM-5** [10] and **UWDM-7** [11] are likely occurring (for full details see the ESM). Most importantly, the reticular design and subsequent expansion of the axle—with or without an interlocked macrocycle—yielded MOFs with identical topologies and the void space sufficient for qualitative indications of robust dynamics.

3 Conclusions

Utilizing the principles of reticular chemistry, robust MOFs have been produced that contain T-shaped linkers, with and without interlocked macrocycles. When the MOF topology contains a free volume large enough to accommodate a full rotaxane linker, dynamic motion of the **24C6** macrocycle could be monitored by ^{2}H VT SSNMR spectroscopy. Most importantly, applying the principles of reticular chemistry produced a pair of isoreticular MOFs **UWCM-14** and **UWDM-14** with the same (lil) framework net. This is the first time it has been possible to create and compare MOFs of the same net, with and without the presence of an interlocked macrocycle and is therefore an important step in the rationale design of robust dynamic materials. We are presently exploring the possibility of applying these same principles of reticular design to the creation of isoreticular MOFs with and without a molecular shuttle capable of linear translational motion inside a porous framework.

Acknowledgements

S. J. L. acknowledges the Natural Sciences and Engineering Research Council of Canada for support of a Discovery Grant (101694) and a Canada Research Chair. R. W. S. is also grateful for support from NSERC, the Canadian Foundation for Innovation, the Ontario Innovation Trust, the University of Windsor for the development and maintenance of the SSNMR centre, and for funding from the Florida State University and the National High Magnetic Field Laboratory (NHMFL), which is funded by the National Science Foundation Cooperative Agreement (DMR-1644779) and by the State of Florida. The authors acknowledge M. Revington for technical assistance with solution NMR spectroscopy and J. Auld for technical assistance with high resolution mass spectrometry.

Electronic Supplementary Material: Supplementary material (full synthetic and characterization details for new linkers including ^{1}H, ^{13}C NMR spectra and high resolution mass spectrometry; synthesis of MOFs and characterization by powder X-ray diffraction (PXRD), TGA; summary of all single crystal X-ray diffraction studies; and SSNMR data) is available in the online version of this article at https://doi.org/10.1007/s12274-020-3123-z. Full details of single crystal X-ray diffraction studies have been deposited with the CCDC as accession numbers 1860136 and 2019453-2019457.

References

[1] Bissell, R. A.; Córdova, E.; Kaifer, A. E.; Stoddart, J. F. A chemically and electrochemically switchable molecular shuttle. *Nature* **1994**, *369*, 133–137.

[2] Bruns, C. J.; Stoddart, J. F. *The Nature of the Mechanical Bond: From Molecules to Machines*; John Wiley & Sons: New York, 2017.

[3] Erbas-Cakmak, S.; Leigh, D. A.; McTernan, C. T.; Nussbaumer, A. L. Artificial molecular machines. *Chem. Rev.* **2015**, *115*, 10081–10206.

[4] Gholami, G.; Zhu, K. L.; Baggi, G.; Schott, E.; Zarate, X.; Loeb, S. J. Influence of axle length on the rate and mechanism of shuttling in rigid H-shaped [2]rotaxanes. *Chem. Sci.* **2017**, *8*, 7718–7723.

[5] Martinez-Bulit, P.; Wilson, B. H.; Loeb, S. J. One-pot synthesis of porphyrin-based [5]rotaxanes. *Org. Biomol. Chem.* **2020**, *18*, 4395–4400.

[6] Zhu, K. L.; Baggi, G.; Loeb, S. J. Ring-through-ring molecular shuttling in a saturated [3]rotaxane. *Nat. Chem.* **2018**, *10*, 625–630.

[7] Wilson, B. H.; Loeb, S. J. Integrating the mechanical bond into metal-organic frameworks. *Chem* **2020**, *6*, 1604–1612.

[8] Martinez-Bulit, P.; Stirk, A. J.; Loeb, S. J. Rotors, motors, and machines inside metal–organic frameworks. *Trends Chem.* **2019**, *1*, 588–600.

[9] Deng, H. X.; Olson, M. A.; Stoddart, J. F.; Yaghi, O. M. Robust dynamics. *Nat. Chem.* **2010**, *2*, 439–443.

[10] Farahani, N.; Zhu, K. L.; O'Keefe, C. A.; Schurko, R. W.; Loeb, S. J. Thermally driven dynamics of a rotaxane wheel about an imidazolium axle inside a metal-organic framework. *ChemPlusChem* **2016**, *81*, 836–841.

[11] Martinez-Bulit, P.; O'Keefe, C. A.; Zhu, K. L.; Schurko, R. W.; Loeb, S. J. Solvent and steric influences on rotational dynamics in porphyrinic metal–organic frameworks with mechanically interlocked pillars. *Cryst. Growth Des.* **2019**, *19*, 5679–5685.

[12] Gholami, G.; Wilson, B. H.; Zhu, K. L.; O'Keefe, C. A.; Schurko, R.; Loeb, S. J. Exploring the dynamics of Zr-based metal-organic frameworks containing mechanically interlocked molecular shuttles. *Faraday Discuss.*, in press, DOI: 10.1039/D0FD00004C.

[13] Chen, Q. S.; Sun, J. L.; Li, P.; Hod, I.; Moghadam, P. Z.; Kean, Z. S.; Snurr, R. Q.; Hupp, J. T.; Farha, O. K.; Stoddart, J. F. A redox-active bistable molecular switch mounted inside a metal–organic framework. *J. Am. Chem. Soc.* **2016**, *138*, 14242–14245.

[14] Vukotic, V. N.; O'Keefe, C. A.; Zhu, K. L.; Harris, K. J.; To, C.; Schurko, R. W.; Loeb, S. J. Mechanically interlocked linkers inside metal–organic frameworks: Effect of ring size on rotational dynamics. *J. Am. Chem. Soc.* **2015**, *137*, 9643–9651.

[15] Zhu, K. L.; Vukotic, V. N.; O'Keefe, C. A.; Schurko, R. W.; Loeb, S. J. Metal–organic frameworks with mechanically interlocked pillars: Controlling ring dynamics in the solid-state via a reversible phase change. *J. Am. Chem. Soc.* **2014**, *136*, 7403–7409.

[16] Vukotic, V. N.; Harris, K. J.; Zhu, K. L.; Schurko, R. W.; Loeb, S. J. Metal–organic frameworks with dynamic interlocked components. *Nat. Chem.* **2012**, *4*, 456–460.

[17] Zhu, K. L.; O'Keefe, C. A.; Vukotic, V. N.; Schurko, R. W.; Loeb, S. J. A molecular shuttle that operates inside a metal–organic framework. *Nat. Chem.* **2015**, *7*, 514–519.

[18] McGonigal, P. R.; Deria, P.; Hod, I.; Moghadam, P. Z.; Avestro, A. J.; Horwitz, N. E.; Gibbs-Hall, I. C.; Blackburn, A. K.; Chen, D. Y.; Botros, Y. Y. et al. Electrochemically addressable trisradical rotaxanes organized within a metal–organic framework. *Proc. Natl. Acad. Sci. USA* **2015**, *112*, 11161–11168.

[19] Yaghi, O. M.; O'Keeffe, M.; Ockwig, N. W.; Chae, H. K.; Eddaoudi, M.; Kim, J. Reticular synthesis and the design of new materials. *Nature* **2003**, *423*, 705–714.

[20] Lin, X.; Telepeni, I.; Blake, A. J.; Dailly, A.; Brown, C. M.; Simmons, J. M.; Zoppi, M.; Walker, G. S.; Thomas, K. M.; Mays, T. J. et al. High capacity hydrogen adsorption in Cu (II) tetracarboxylate framework materials: The role of pore size, ligand functionalization, and exposed metal sites. *J. Am. Chem. Soc.* **2009**, *131*, 2159–2171.

[21] Yan, Y.; Yang, S. H.; Blake, A. J.; Schröder, M. Studies on metal–organic frameworks of Cu(II) with isophthalate linkers for hydrogen storage. *Acc. Chem. Res.* **2014**, *47*, 296–307.

[22] Lin, X.; Jia, J. H.; Zhao, X. B.; Thomas, K. M.; Blake, A. J.; Walker, G. S.; Champness, N. R.; Hubberstey, P.; Schröder, M. High H_2 adsorption by coordination-framework materials. *Angew. Chem., Int. Ed.* **2006**, *45*, 7358–7364.

[23] Cai, J. F.; Lin, Y. C.; Yu, J. C.; Wu, C. D.; Chen, L.; Cui, Y. J.; Yang, Y.; Chen, B. L.; Qian, G. D. A NbO type microporous metal–organic framework constructed from a naphthalene derived ligand for CH_4 and C_2H_2 storage at room temperature. *RSC Adv.* **2014**, *4*, 49457–49461.

[24] Noujeim, N.; Zhu, K. L.; Vukotic, V. N.; Loeb, S. J. [2]Pseudorotaxanes from T-shaped benzimidazolium axles and [24]crown-8 wheels. *Org. Lett.* **2012**, *14*, 2484–2487.

[25] Kilbinger, A. F. M.; Cantrill, S. J.; Waltman, A. W.; Day, M. W.; Grubbs, R. H. Magic ring rotaxanes by olefin metathesis. *Angew. Chem., Int. Ed.* **2003**, *42*, 3281–3285.

[26] Akimbekov, Z.; Katsenis, A. D.; Nagabhushana, G. P.; Ayoub, G.; Arhangelskis, M.; Morris, A. J.; Friščić, T.; Navrotsky, A. Experimental and theoretical evaluation of the stability of true MOF polymorphs explains their mechanochemical interconversions. *J. Am. Chem. Soc.* **2017**, *139*, 7952–7957.

[27] Dolomanov, O. V.; Bourhis, L. J.; Gildea, R. J.; Howard, J. A. K.; Puschmann, H. *OLEX2*: A complete structure solution, refinement and analysis program. *J. Appl. Crystallogr.* **2009**, *42*, 339–341.

[28] Spek, A. L. *PLATON SQUEEZE*: A tool for the calculation of the disordered solvent contribution to the calculated structure factors. *Acta Crystallogr. C Struct. Chem.* **2015**, *71*, 9–18.

[29] Barthel, S.; Alexandrov, E. V.; Proserpio, D. M.; Smit, B. Distinguishing metal–organic frameworks. *Cryst. Growth Des.* **2018**, *18*, 1738–1747.

[30] Blatov, V. A.; Shevchenko, A. P.; Proserpio, D. M. Applied topological analysis of crystal structures with the program package ToposPro. *Cryst. Growth Des.* **2014**, *14*, 3576–3586.

[31] Mondloch, J. E.; Bury, W.; Fairen-Jimenez, D.; Kwon, S.; DeMarco, E. J.; Weston, M. H.; Sarjeant, A. A.; Nguyen, S. B. T.; Stair, P. C.; Snurr, R. Q. et al. Vapor-phase metalation by atomic layer deposition in a metal–organic framework. *J. Am. Chem. Soc.* **2013**, *135*, 10294–10297.

[32] Barbour, L. J. Crystal porosity and the burden of proof. *Chem. Commun.* **2006**, 1163–1168.

[33] Smith, J. V. Topochemistry of zeolites and related materials. 1. Topology and geometry. *Chem. Rev.* **1988**, *88*, 149–182.

[34] Zhang, J. P.; Zhang, Y. B.; Lin, J. B.; Chen, X. M. Metal azolate frameworks: From crystal engineering to functional materials. *Chem. Rev.* **2012**, *112*, 1001–1033.

[35] Gole, B.; Bar, A. K.; Mallick, A.; Banerjee, R.; Mukherjee, P. S. An electron rich porous extended framework as a heterogeneous catalyst for Diels–Alder reactions. *Chem. Commun.* **2013**, *49*, 7439–7441.

[36] Cai, J. F.; Yu, J. C.; Wang, H. L.; Duan, X.; Zhang, Q.; Wu, C. D.; Cui, Y. J.; Yu, Y.; Wang, Z. Y.; Chen, B. L. et al. A noninterpenetrated metal–organic framework built from an enlarged tetracarboxylic acid for small hydrocarbon separation. *Cryst. Growth Des.* **2015**, *15*, 4071–4074.

[37] Cai, J. F.; Yu, J. C.; Xu, H.; He, Y. B.; Duan, X.; Cui, Y. J.; Wu, C. D.; Chen, B. L.; Qian, G. D. A doubly interpenetrated metal–organic framework with open metal sites and suitable pore sizes for highly selective separation of small hydrocarbons at room temperature. *Cryst. Growth Des.* **2013**, *13*, 2094–2097.